Improvements in the physical modelling of tsunamis and their effects

William Allsop[1], Ian Chandler[2], Mario Zaccaria[3]

(1) Technical Director, (2) Engineer, (3) Visiting Researcher; HR Wallingford, Wallingford, OX10 8BA, UK.
(Email (1) w.allsop@hrwallingford.com, (2) i.chandler@hrwallingford.com)

Proceedings of the 5th International Conference on The Application of Physical Modelling to Port and Coastal Protection, Coastlab14, Varna, Bulgaria, 29 September – 2 October 2014.

Abstract

This paper summarises a series of advances in the development, testing and use of a novel pneumatic Tsunami Generator for physical models. It describes the main principles behind the initial development and use of the HR Wallingford/UCL Tsunami Generator, then describes various stages of further modelling and testing to improve and extend a numerical model of its performance. Tests on a (slightly) improved device are presented, including the successful generation of the 15 min long Mercator time series from the 2004 Indian Ocean tsunami, and trials of the 2011 Tohoku tsunami.

Keywords: Tsunamis, physical modelling, numerical modelling, coastal engineering

1 Introduction

Tsunamis are very long-period (10-30 minute) waves caused (primarily) by sub-marine seabed movement. They are relatively rare phenomena, but can be extremely destructive. They may be driven by sub-sea seismic action or landslides; by sub-aerial landslides, or by volcanic action. Whilst tsunamis caused by point sources may be highly destructive locally, their intensity radiate out, reducing with distance. In contrast, seismic action along a subduction zone (e.g. the 2004 Indian Ocean Boxing Day event, or the 2011 Tohuko earthquake) may cause a long length (or several parts) of fault to move, causing a longer wave front which reduces less with distance than from a point source, so potentially more damaging to coastlines near or far. A notable feature of some tsunamis, notably those on the 'upward' side of a subduction zone, is the initial depression or trough that precedes the main wave. Trough-led tsunamis may be particularly destructive to coastal structures due to the 'perched' phreatic surface left behind within the shoreline or coastal defences, and/or due to the debris carried by the (returning) incoming wave.

It is important to plug gaps in the knowledge of characteristics of tsunamis in the nearshore and onshore regions, where their impact on coastal communities is difficult to predict because of the rarity of in-situ measurements. If properly conducted, numerical and physical simulations can help to obtain the missing information. To date, the majority of physical experiments worldwide have been limited to generation of solitary waves as an approximation for tsunami. These leave much to be desired, particularly failing to reproduce tsunami wavelengths and flow durations. Further limitations come from their inability to reproduce trough-led long waves, a frequent characteristic of tsunamis. In theory, paddles can generate trough-led

waves by starting with the piston part-stroke, and pulling it back. This is not however without a number of substantial attendant difficulties.

Previous work born of collaboration between University College London (UCL)'s Earthquake and People Interaction Centre (EPICentre) and HR Wallingford developed the original Tsunami Generator for use in physical model testing of shoreline and inundation processes.

Within HYDRALAB-IV (http://www.hydralab.eu/), HyReS topic 9.1.2 "Wave generation for tsunami wave groups" was a Joint Research Activity to improve the generation of tsunami waves, specifically to:

- Obtain new information on example time series of tsunamis;
- Develop an advanced CFD model to emulate the behaviour of the Tsunami Generator;
- Conduct tests to benchmark and extend physical modelling capabilities.

This work discussed here has therefore been conducted in three main phases. The original development of the Tsunami Generator was led by HR Wallingford supported by Dr Tiziana Rossetto of UCL in 2008-2011. Testing using this device formed the main part of the PhD work by Charvet (2011). Following those initial studies, Visiting Researchers at Wallingford collected data on the 2011 Tohoku tsunami, and developed an initial CFD model of the Tsunami Generator. That CFD model was then refined and used to benchmark key aspects of performance, develop and test modifications to the Tsunami Generator itself. A modified version of the Tsunami Generator was then re-tested in a short series of further flume experiments, culminating in the successful generation of the 2004 Mercator time signal at 1:50 scale.

That work will then be extended during 2014 under a further UCL / HR Wallingford project, URBANWAVES, which will include the development of a new (and larger) Tsunami Generator.

This paper therefore summarises material from previous work, particularly: information on tsunami data gathering; and results from the first physical and numerical experiments on the Tsunami Generator. It illustrates how the CFD model was developed and describes tests to select the best mesh to use. It then describes the path to re-create real tsunami traces. Finally it introduces the changes made to the Tsunami Generator (tested numerically) to improve its precision and performances, and describes the physical model tests with the adapted Tsunami Generator. It details how the model was set-up and shows how physical experiments were conducted. Results are presented for general capability tests, run to explore the limits to wave generation, and for real tsunamis reproduction.

2 Background

2.1 Tsunami signals

The quality of any simulation depends strongly on the input wave signal, both for numerical and physical modelling. A number of different attempts have been made to determine tsunami wave forms. Approaches include using generic wave signal such as solitary or N-waves, or modelling a specific wave event.

The most common model used to describe a non-periodic wave is the solitary wave, or soliton, a shallow water wave that consists of a single displacement of water above the mean water level. Hammack (1972) showed how a positive initial surface disturbance will eventually decompose into solitons, and this conclusion has been used to justify the use of solitons to model tsunamis. Madsen *et al* (2008) have however argued that the assumptions this solution implies may not be relevant to geophysical tsunamis.

2.1.1 Solitary and N-waves

Tadepalli & Synolakis (1994) proposed to replace the solitary wave with N-shaped solitary-like wave, which can be either leading depression N-waves (LDN) or leading elevation N-waves (LEN). The generalized N-wave is given by:

$$\eta(x,0) = \alpha H(x - x_2)\mathrm{sech}^2\left(k(x - x_1)\right)$$

where $k = \frac{1}{h}\sqrt{\frac{3H}{4h}}$, α a scaling parameter to allow comparison with solitary waves, x_1 and x_2 define the locations of trough and crest.

Their work was supported by accounts of wave recession before the arrival of the tsunami wave in Indonesia 1992, Nicaragua 1992, Philippines 1994, Mexico in 1995 or Thailand in 2004. Tadepalli & Synolakis (1994) suggested that the nature of the sea floor deformation in subduction zones leads to LDN waves on the subsiding plate, whereas LEN waves travel away from the sub-duction zone towards the open ocean. They also found that N-waves with a trough first (LDN) run-up higher than crest-led N-waves (LEN). LEN waves nevertheless have higher run-ups than their equivalent solitary waves.

2.1.2 Time series

An inherently more realistic option is to base a simulation on an incident wave as recorded during a known tsunami event. Ideally, a clean signal should be obtained in a nearshore area, and on the direct trajectory of the tsunami, and to avoid noise and distortion due to local effect and reflections. Such requirements are however seldom met!

The 2004 Indian Ocean tsunami, despite the great media coverage, gave very few clean records of the wave form, as the Indian Ocean was equipped with virtually no warning or (tsunami) wave recording devices. By far the best time series obtained was the 'Mercator' signal, recorded by a Belgian yacht anchored 1.6km off the coast of Phuket (Thailand). The boat rode the 4m-high wave without damage. The depth-sounder recorded the depth variation giving a record of the local depth, hence surface elevations.

As visible in Figure 1, the train of waves recorded was trough-led (-2.77m) and includes following peaks, although these further oscillations may be strongly influenced by reflections from the shoreline.

The 'Mercator' signal is still the closest to a generic recording of the 2004 Indian Ocean Tsunami. It is likely that the last two waves were significantly modified by reflections from the coast and were travelling in the opposite direction, so only the first part of the signal has been used in the studies here. Significant parameters of the main wave (respectively: wave height, crest amplitude, trough amplitude and wavelength) are the following: H=6.5m, a_{crest}=3.7m, a_{trough}=2.8m, and L=14400m, Rossetto *et al* (2011).

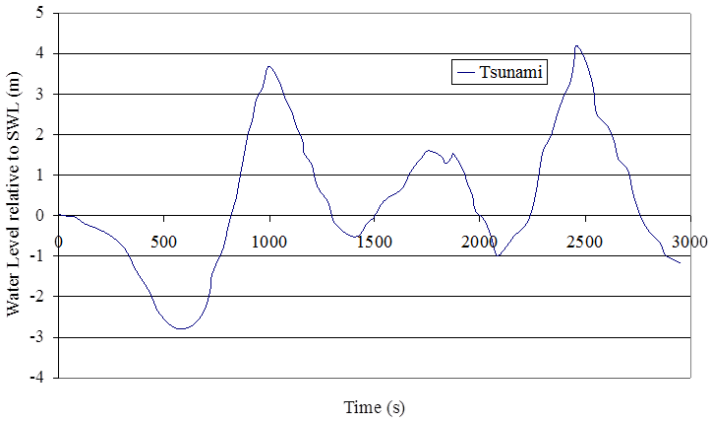

Figure 1: Signal recorded by the Mercator yacht

2.1.3 Tide gauges

A few days after the 11 March 2011 Tohoku tsunami hit the coast of Eastern Japan, Japan Meteorological Agency (JMA), Maritime Safety Agency and Central Research Institute of Electric Power Industry (CRIEPI) published data from tide gauges. All of those facing directly into the rupture zone were damaged by the wave and stopped recording as the wave exceeded their measurement limit. Others to north or south nevertheless give some useful information about form and arrival time of the first wave.

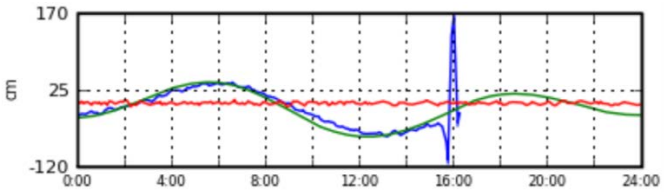

Figure 2: Hachinohe Tide Gauge Signal on 11 March 2011 (from CRIEPI)

At Hachinohe, some 350km north of Fukushima Daiichi Nuclear Plant, the tide gauge recorded the arrival of the tsunami wave. Raw data show that the first wave of about 1.70m was preceded by a 0.9m trough, Figure 2. Hachinohe is a rare example of a port where the tide gauge was able to record the shape of the first wave. Most gauges, like the one in Ofunato (200km north of Fukushima Daiichi) went off-scale when the first peak arrived. Nevertheless it can be inferred that a 0.8m trough reached Ofunato before the first crest. Gauges located outside of the direct trajectory of the tsunami were exposed to waves of smaller height which were entirely recorded. The gauge at Choshi (about 180km south of Fukushima Daiichi) recorded a crest 1.74m above normal sea level, but with no sign of a leading trough.

On 28 March 2011, the Earthquake Research Institute of Tokyo University (ERI) displayed on their website http://outreach.eri.u-tokyo.ac.jp/eqvolc/201103_tohoku/eng observation records from Ocean Floor Cable Seismometers. Two of those ocean bottom pressure gauges were situated close to the rupture zone of the earthquake off the Tohoku coast. These pressure gauges recorded sea level that followed the seismic event.

According to ERI, TM1 is set about 76km away from the Japanese coast, in 1600m depth. The other pressure gauge (TM2) is 47km away from land, in 1000m of water. The location of the gauges and the estimated epicentre of the M9.0 earthquake are shown in Figure 3a.

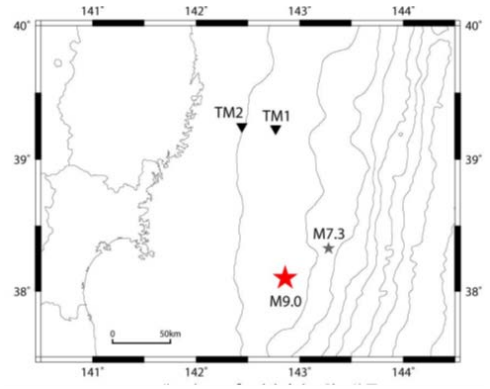

Figure 3a: Location of the Ocean Bottom Pressure Gauges TM1 and TM2 (from ERI)

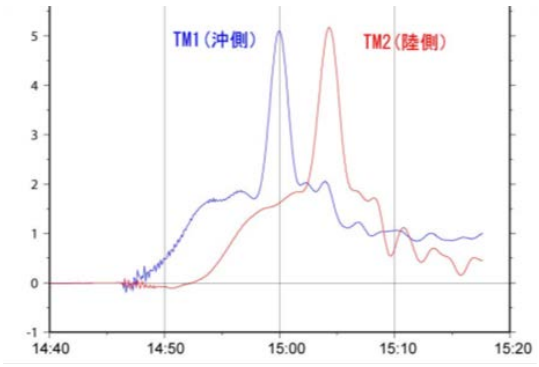

Figure 3b: Ocean Bottom Pressure Gauge records from 11 March 2011 (from ERI)

The two signals recorded by pressure gauges TM1 and TM2 (Figure 3b) show the sea level rising by 2m over about 10 minutes. Then a second major wave reached TM1 ~11 minutes later, causing an additional 3 metre rise. TM2, 30km further landward, recorded the same (composite) wave with a 4min delay. These signals give essential information about the wave shape on the western side of the earthquake. The wave shape was almost the same for both gauges, with only a slight time delay. This suggests that these signals may be taken as the most generic recording of the March 2011 Tohoku tsunami. Later analysis suggests that two seafloor movements caused the 20 minute long 2m high wave, and then the abrupt 3m rise. It is this composite motion that has triggered consideration in Japan since this event of multiple-excitation tsunamis. The time series extracted from TM2 has been used here for both numerical and physical experiments.

The Port and Harbour Bureau of Ministry of Land, Infrastructure, Transport and Tourism (MLITT) has several GPS buoys along the coast of Japan), six of which faced the rupture zone. These buoys provide time series in several locations along the Eastern Coast of Japan, located about 10-20km off the coast, set in 100-300m deep water. Propagation from the rupture zone (depth>1000m) to the continental shelf (depth<200m) had already modified them by shoaling.

The perturbation caused by the earthquake is visible on most of these records (14:46 JST). A small trough (about 0.5m) is visible before the first crest and the main peak (about 5m), which matches the signals discussed earlier. The peak was then followed by a major trough (~3m) in locations directly facing the rupture zone.

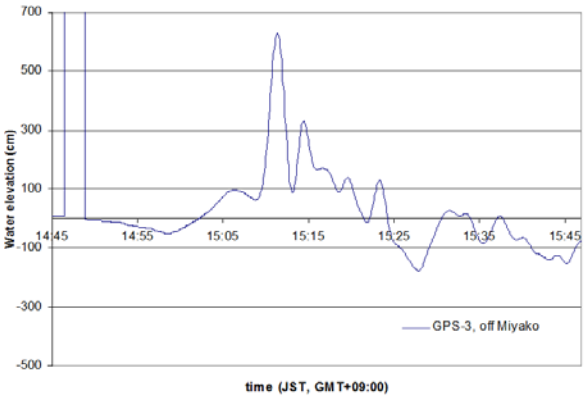

Figure 4a: Signal off Miyako (GPS-3)

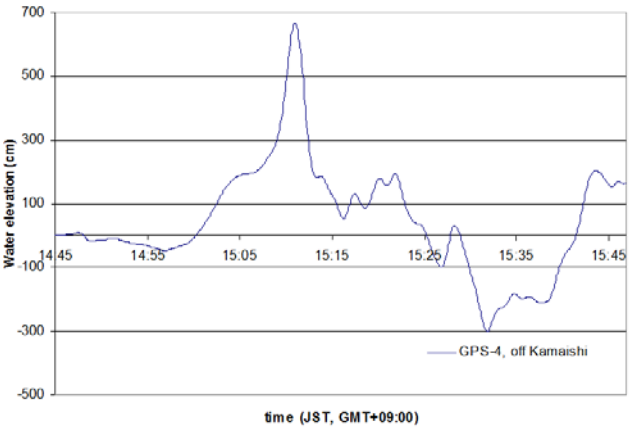

Figure 4b: Signal off Kamaishi (GPS-4)

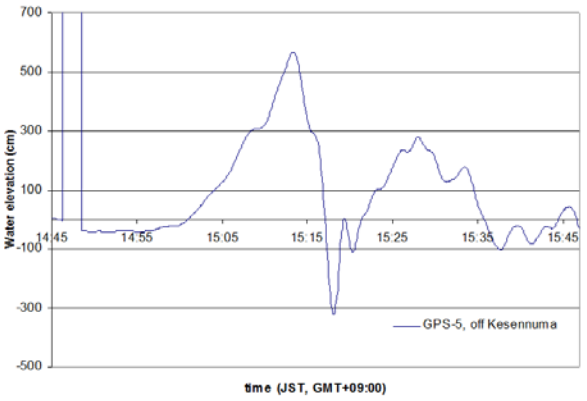

Figure 4c: Signal off Kesennuma (GPS-5)

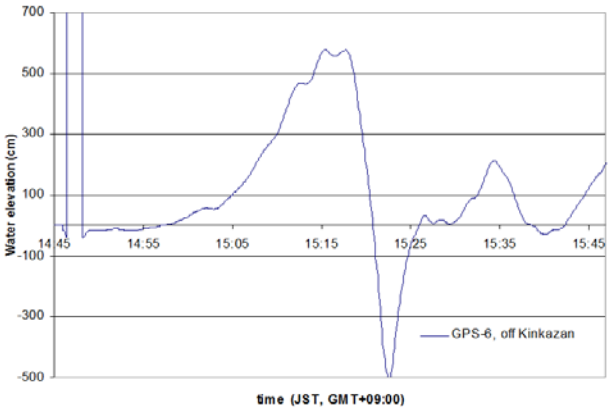

Figure 4d: Signal off Kinkazan (GPS-6)

2.2 Physical modelling

2.2.1 Tsunami generation by wave paddles

Historically, laboratory tests evolved independently from analytical studies. Hall & Watts (1953) generated long waves over a constant depth area, then climbing up a uniform sloping beach, analogy for a flat-bottomed ocean and sloping continental shelf. The waves resembled solitary waves as defined by Russel (1845). Wiegel (1955) modelled landslide-generated waves by a wedge-shaped box sliding down a plane. The “moving block” method is still the most common way of modelling landslide waves.

Through the years, solitary waves have been generated in laboratories using horizontally-moving paddles. In 1972, Hammack used a short section of flume floor that could be raised or lowered to reproduce seafloor motion. Potentially the best way to simulate effects of sub-sea bed movement, this approach does not however appear to have been repeated since.

Nowadays, a whole range of wave generation methods are used, depending on the facilities available and the objectives of the study. Thunsyanthan & Madabhushi (2008) generated some form of wave (about 0.1m high, 1.5s period) by dropping a 100kg rectangular block (free-fall) into the water at the deeper end of a very short (4.5m) flume. Those waves, equivalent to H=2.5m, T=7.5s at 1:25 scale, will have been relatively poorly controlled and bear very little similarity with realistic tsunami waves.

Conventional wave generation uses piston-driven paddles. At Port and Airports Research Institute in Japan (PARI), a 184m-long, 3.5m-wide and 12m-deep “Large Hydro-Geo Flume” was described by Shimosako et al (2002). Waves up to Hs = 1.4m at T=5.5s, Hmax ≤ 3.5m high for a 6-8s period and a 7.6m depth are generated by a piston wave-maker. [The wave period capacity may have been increased in recent years.] At Oregon State University, a multi-directional Tsunami Wave Basin, 48.8m by 26.5m with a 2m depth, uses sliding-wedge wave paddles to generate solitary waves up to a 0.8m height, Yim et al (2009).

Piston and wedge wave generators have been used for many years, so their use and limits are well-known. The characteristics of the wave they can generate are limited by depth and paddle stroke. The difficulties in generating true tsunami waves are their extremely long wavelengths (~500km). No conventional paddles has a stroke long enough to generate such wavelengths.

Finally, many tsunami waves are complex combinations of waves that may start with a receding water level. Producing trough-led wave trains is particularly difficult with conventional paddles. Probably, the only way they could generate a trough-led wave is for the piston to start part-stroke and then be pulled back in its first cycle. But this method has not been shown to produce stable wave forms as highlighted by the experimental results of Schmidt-Koppenhagen *et al* (2006).

2.2.2 Pneumatic generation

In 2008, a new pneumatic Tsunami Generator was developed by HR Wallingford supported by UCL. Historically, hydraulics laboratories used pneumatic tide generators to move large amounts of water in models of tidal estuaries. This makes them ideally suited to the generation of tsunamis because they are capable of creating the unusually long wavelengths that characterise tsunamis.

Penchev (2009) used a ‘collapsing water column’ technique, lifting water using vacuum pressure and releasing it abruptly to reproduce a simple 'crest-led tsunami. The water release was gravity-driven and otherwise uncontrolled so the wave profile could not be changed.

Allsop *et al* (2008), Rossetto *et al* (2009), Robinson (2009, 2010) and Charvet (2011) describe the working of the new wave generator and the first stages of testing to verify its capacities and limitations. They showed that the new Tsunami Generator had reproduced solitary waves and N-waves with large wavelengths, and a shortened simulation of the 2004 Indian Ocean Tsunami as recorded off the coast of Thailand (“Mercator” trace). This device allowed for the first time the stable simulation of extremely long waves led either by a crest or a trough (depressed wave).

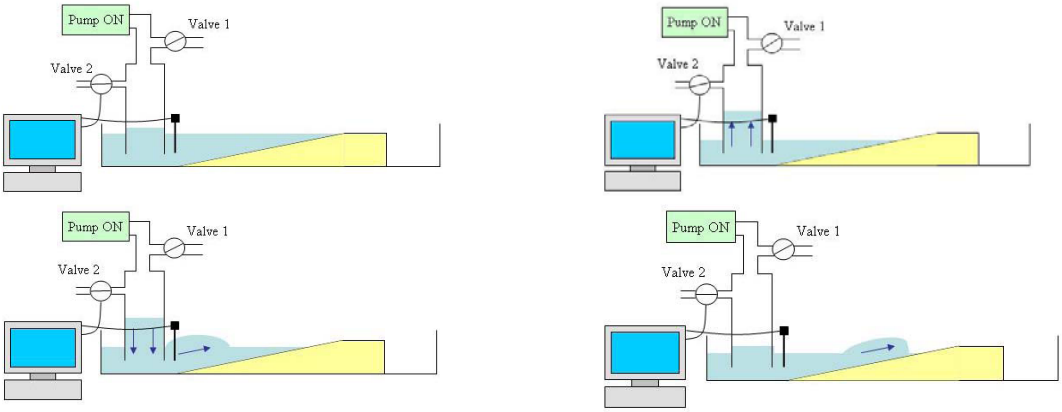

Figure 5: Schematic drawings that describe the operation of the Tsunami Generator during a trough-led wave generation, after Robinson (2009)

An inverted tank sits at one end of a long flume, with a submerged opening (outlet) facing into the active part of the wave flume. A fan (permanently operating when the generator is in use) extracts air from the top of the tank, drawing water from the test flume into the Tsunami Generator tank. This is then released under control to generate a wave. An air valve in the top of the tank is controlled through a computer to give the desired wave shape. A schematic drawing of the conceptual design is shown in Figure 5.

The starting position (a) for the Tsunami Generator will be with vacuum pump on, (safety) Valve 1 slightly open and (control) Valve 2 fully open. The water in the tank will be stable and higher than the initial flume water level. Valve 2 will then close (b) under the control of the computer, and the water level in the tank will begin to rise, creating the leading trough. Then (c) Valve 2 will be re-opened under control, and the wave crest is created. At all times the pump will be on and (safety) Valve 1 remains slightly open. Eventually (d), Valve 2 will return to its original position and the sequence ends. If the flume is long enough, then the wave will continue to propagate away from the generator.

This Tsunami Generator was intended to generate tsunami at scales between 1:50 and 1:150, using undistorted Froude scaling.

During 2009-2010, tests at HR Wallingford were performed by UCL researchers Charvet, Robinson and Lloyd to evaluate the Tsunami Generator's performance characteristics. The validation tests included the generation of sine waves for model periods ranging from 50s to 200s. Other more complicated profiles such as solitary waves and N-waves were also produced. Studies by Allsop et al (2008), Rossetto et al (2009) had already shown that this new tsunami generating device could produce the desired wave shapes, including trough-led waves, with consistent repeatability. Those initial tests did not however develop enough information to allow re-design of the device to extend its performance

Further tests investigated the flow around, forces and pressures exerted on an idealised building (simulating an apartment block or hotel) when inundated by a tsunami. Initial testing was performed on a simple slope to observe tsunami flow velocities inland. Weighted foam buildings were then used to look at the flow around coastal buildings and the forces being exerted on them during inundation. Finally, model building structures were used to measure pressure distributions and whole body forces on the buildings during inundation.

3 Numerical modelling

3.1 Stage 1

In 2011, Barthel built a 2-dimensional (2D) numerical model to emulate the behaviour of the original Tsunami Generator to assess its quality (reliability / comprehensiveness / robustness), and then to model different wave profiles, perhaps also different device geometries. The model was developed using the OpenFOAM® computational fluid dynamics (CFD) platform and uses the original Tsunami Generator length and height, 4.8m and 1.8m respectively (width is not included in a 2D model). Using this model, Barthel reproduced many of the waves generated in 2009 physical modelling, and ran solitary waves to study their propagation and shoaling. Finally she used the model to investigate the limits of the generator, in particular the maximum achievable height for a generated wave and the maximum steepness the tank could generate.

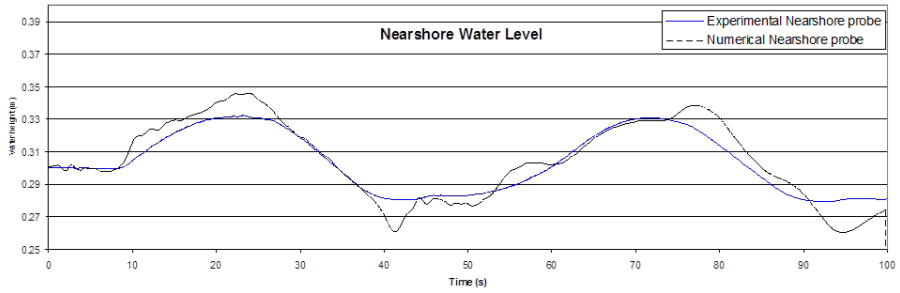

Figure 6: “Nearshore” Flume Water level for a 50s sine wave (model)

A set of "sine wave" tests were run to explore whether the numerical model could follow a target signal and produce a specific waveform. The wave periods used ranged between 50s and 200s (model periods). Elevations from the model were plotted for each test and compared to the water elevations measured experimentally, see Robinson (2009), as in Figure 6. The agreement between experimental and simulated wave generation was good, although the numerical model carried more high frequency components.

Then, a number of 'solitary' waves were generated as many previous researchers have published results for solitary waves. These tests suggested that producing a steep wave could lead to the generation of a train of small crests following the main wave, perhaps a particular limitation of the generator. For particularly rapidly rising target signals, the water could not be released from the tank as fast as required for such a short duration wave, possibly limited by resistance at the tank outlet.

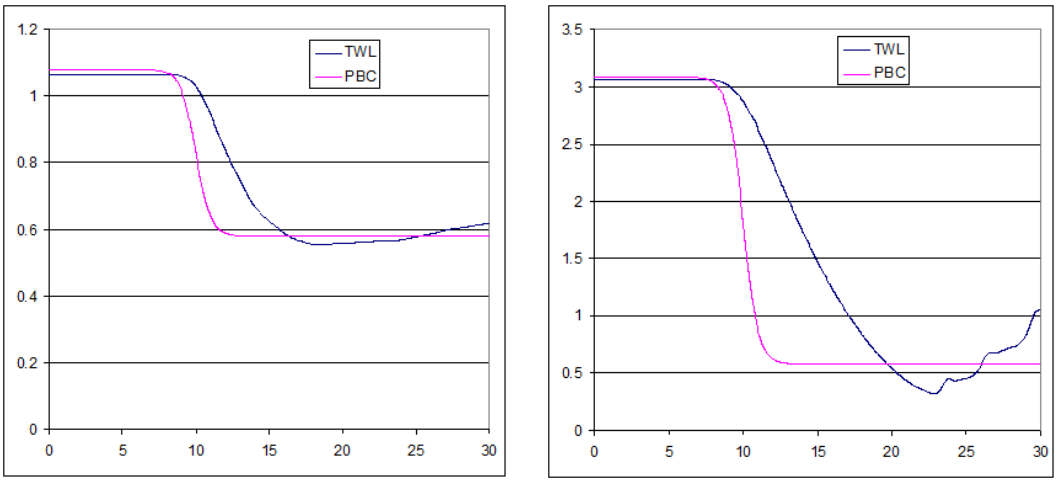

Figure 7: Tank Water Level (TWL) and Pressure Boundary Condition (PBC) in a free release for a 0.5m (a) and a 2.5m (b) head difference (note different vertical scales)

Another limitation was the maximum height the generated wave could attain, in that increasing the target signal didn't necessarily lead to an equivalent increase in wave elevation. As the steepness of the wave increased, the wave was not fully generated, but separated in a series of sharp peaks. This again suggested a limit to the outflow rate caused by throttling at the outlet. This issue was further explored through studying the Tank Water Level (TWL). A series of "free release" tests were run for different head differences (between tank and flume water level), and Figure 7 shows two examples of those tests.

3.2 Stage 2

Following exploratory work in 2011, the next stage in 2012 was to adapt / improve the OpenFOAM® numerical model of the Tsunami Generator, and thus to provide a tool to extrapolate the current design to revised geometries, and to new tsunamis time series.

Several grid independence tests were performed to validate the mesh before revising the geometry and studying nre tsunami traces. Grid independence tests provided information about the reliability of the mesh, and indicated if the number of cells within the domain was enough. Once the model was validated, a transfer function between movement of water in the tank, and the heights of the generated waves was investigated, giving approximate limits to the capabilities of the tank. This function remained a guide only to these capabilities, because other important parameters like the length of the waves and the required volumes have a strong influence in the process of tsunami generation.

The last phase of that study focused on finding an improved shape for the outlet lip of the tank to eliminate surface disturbances and back-eddies at the mouth of the tank (indicating un-wanted energy losses), and thus to improve outlet flow rates for a given head in the tank. Simulations run with this reshaped lip tested the efficiency of the new profile. Different sizes and shapes of the outlet were designed and tested and different geometries of the flume where built as well to represent: a) the different bathymetries in summer 2012, and previously in 2010; b) a geometry without any slope for the generation of sine waves, which needed to propagate unmodified through the flume.

The wave generation of the numerical model is pressure driven. The model is initialised with a head difference between tank water level (TWL) and flume water level (FWL). For t>0s, the pressure P is regulated by a Boundary Condition (BC) tool assigned to the roof of the tank, which allows us to impose a pre-defined pressure / time profile. Changes in pressure (regulated by this BC) make the water in the tank rise or fall, thus leading to the generation either of troughs (with suction) or crests (with release) into the flume. The use of the pressure condition means that air flows out through the fan and back in through the control valve (driving air pressure changes in the tank) are simplified through the imposition of the pressure boundary condition at the tank roof. Changes to this pressure boundary condition lead to the rise or the fall of the water into the tank and thence to the generation of troughs and crests into the flume.

Beyond the boundary condition assigned to the roof of the tank, the conditions chosen for the solid surfaces (walls of the tank and seabed) are full-slip. Inside the flume (outside of the TG tank), the conditions are those of free surface flow with atmospheric pressure in the top layer of air. At the far end of the flume the geometry is adapted to avoid reflection of tsunamis from the end of the flume, replicating the effect of a sump into which water can fall.

3.3 Setting up and initial experiments

3.3.1 Geometries

The Stage 2 numerical model followed the general settings of the Stage 1 model, but some changes were needed. The geometry modelled was changed to represent the then current bathymetry. The original UCL tests (2009) used a single slope (1/20) which reached a height of 0.7m above flume floor. For the HYDRALAB modelling in 2012, a bathymetry formed by two slopes was used, 1/12 for the initial slope from deep(er) water, then 1/100 representing the nearshore region, reaching a horizontal bed at 0.44m (0.34m after the first slope).

In Stage 1, the Flume Water Level (FWL) had been set at 0.58m, but this was too high to be applied to the new model as a dry flat area was required for the tsunami to propagate inland. This fixed the max FWL for 2012 at 0.40-0.44m, the same level as the model bathymetry. This then forced the outlet level to be revised downward from 0.4m to 0.25m high.

The last difference from the Stage 1 model was the shape of the outlet. Initially the metal sheet had been terminated in a small circle, but this had been omitted in the numerical model, leaving the metal edge exposed to flow. For Stage 2, the circular finisher was faithfully represented, since one of the aims of the study was to identify potential improvements to the tank, included the design of a new flow shaper.

The geometry used in the majority of the Stage 2 simulations is schematised in Figure 8. On the left there is the tank with its circular outlet lip, a flat area representing the zone of constant depth, then the approach slope in the centre, and a slope of the coastal area on the right.

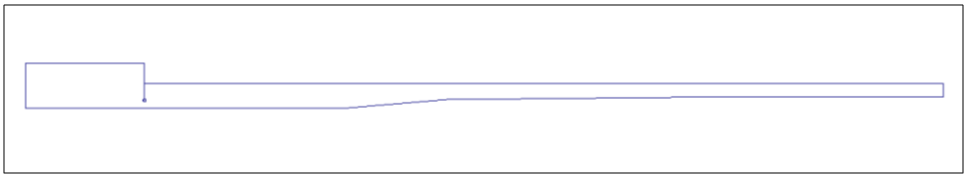

Figure 8: Schematic of tank and flume geometry used for the numerical simulation (geometry 3)

3.3.2 Generic tsunami signals

There are several ways to provide an input to the pressure boundary condition, as time series (or time series functions) where pressure varies with time. An approach explored in Stage 2 was to use the super-imposition of hyperbolic tangents, allowing separate control over the trough and the crest, see example in Figure 9. Each hyperbolic tangent is regulated by three parameters plus the elapsed time:

- a (amplitude of the tanh [m])
- l (regulates the steepness of the curve)
- de (x-coordinate for the inflection point [s])
- time (elapsed time of the simulation [s])

Parameter “a” is assigned depending on the desired range of water movement into the tank.

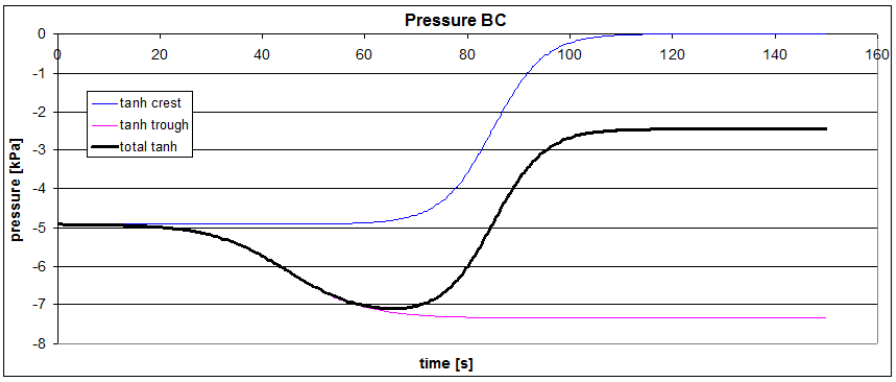

Figure 9: Example pressure boundary condition from super-imposition of hyperbolic tangents

3.3.3 Grid independence tests

In numerical modelling, results should not be significantly influenced by the mesh used. A coarse mesh can lead to an inaccurate calculation, but a fine mesh model may run too slowly, and may suffer instabilities. The aim must always be to run with a mesh just fine enough, so it is important to check whether the results are independent of mesh density. Use of up to six meshes were explored.

The differences in output (error) between two meshes was assessed qualitatively by comparing pressures for a long N-wave simulated on each mesh. The coarser meshes systematically under-estimated pressures in shallow water areas. Graphs of wave pressure against time for fixed flume positions in Figure 10 show that where the water is deeper (x=5m, close to the tank) the values for each mesh follow the same trend during the whole process. There is greater mis-match on the slope where the water is shallow, during both the trough and after the tail of the crest (when the water drops again). Over the wave crest (when the water is

higher) agreement between results for the different meshes is restored. Similar inferences can be drawn from analysis of dynamic pressures in space at a fixed time step.

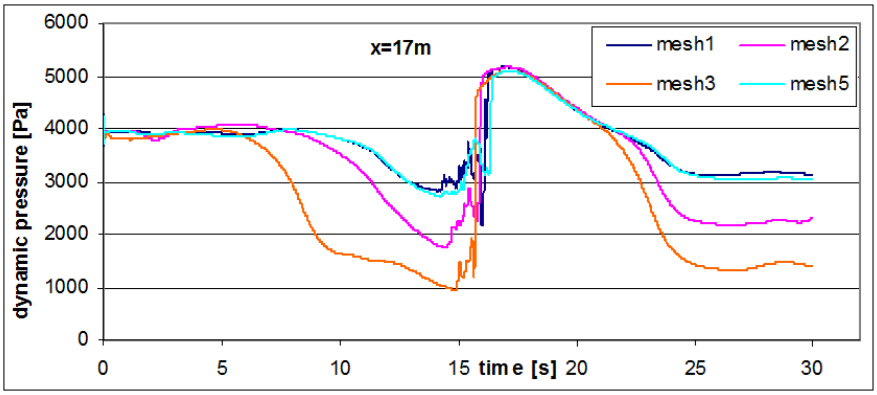

Figure 10: Comparison between meshes: dynamic pressure against time at 17m from the back of the tank (simulations G3.M(nºmesh).W3.cl_1)

These tests suggested that meshes 2, 3 and 4 were too coarse and therefore unreliable. Meshes 1 and 5 seemed to be almost equal. A full grid independence test should begin with a coarse mesh, then increasing systematically the number of cells, until the error between results from steps n and n+1 to become smaller than (say) 1%, or a little more if computation time gets too long (a compromise between mesh definition and calculation time is always necessary).

Qualitative analysis of free surfaces showed good agreement, the only exceptions being close to the mouth of the Tsunami Generator, and locations of wave breaking. A quantitative study was conducted to quantify the error between surface elevations for the two meshes. The obtained results were used to calculate the error against distance along the flume.

Ignoring peak values on the slope where waves break (this study was not to reproduce wave breaking), the errors fall between 0-6%. This percentage is higher than the 1% preferred for assessing independency of mesh size, but as anticipated, compromises between mesh refinement and calculation time are sometimes necessary. Mesh 1 was chosen to continue the research, Figure 11 shows the tank and the grid refinement at the outlet. The main interest was focused on the outlet, and a weakness of the early meshing tool was that refinement in one point affects the whole domain in vertical and horizontal direction from that point. The bottom part of the tank was therefore much more refined than needed. In the main part of the flume, the grid was mostly uniform, until the approach slope. On the slopes, the grid kept the same number of cells vertically, but the cells were squeezed vertically since the upper boundary of the domain (atmosphere) didn't rise with the bathymetry.

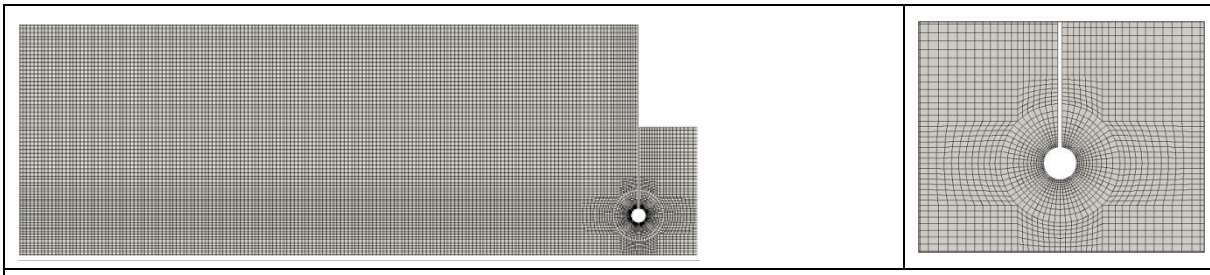

Figure 11: Tank and outlet (geometry 3 – mesh1)

3.4 Transfer function experiments

One of the hopes for Stage 2 was to generate generic transfer functions to link the pressure boundary condition to the generated waves by an appropriate transfer function. For this purpose a new geometry without slope was created and a number of sine waves were simulated, thus limiting the parameters (only period and wave height). Generation of the first sine waves suggested potential sloshing within the tank which badly affected the results at some frequencies. The tank, in fact, acts just like a short basin with its oscillation period, resonating when the period of a generated wave matches the natural period.

To remedy this, the numerical model was modified by inserting baffles (as in the original tank, but absent in previous geometries of the numerical model) to smooth out the sloshing. It was also seen that waves reflected from the flume end after about 30 seconds of simulation, even if a numerical damper was created at the end of the flume. This suggested that a longer flume might be needed to develop a generic transfer function. In fact, tsunamis (at the projected model scales) are several tens of seconds long (even more than 100s), far too much for the flume currently available. In spite of these problems, this initial work provided useful ideas for appropriate transfer functions.

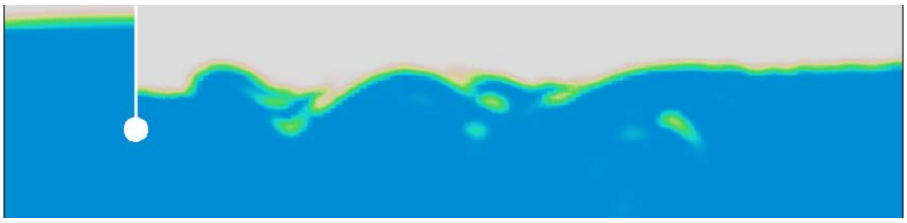

Figure 12: Disturbances at the outlet during generation of a crest (simulation G1.M1.W3.il_1)

Through most of the experiments discussed above, the simulations showed disturbances at the outlet, strongly increasing at higher velocities. Rapid flows detached from the outlet lip during strong outflow - wave generation. This caused separations of flow from the relatively still upper water area and to generation of back-eddies which propagated from the outlet into the flume (Figure 12). These suggest undesired energy losses which will affect wave generation. It was therefore decided to modify the tank outlet with a flow shaper intended to reduce flow discontinuities, and thus energy losses. An image from the numerical model shows a distinct vena contracta from a simulation of a 160s N-wave, Figure 13. The shape of the flow shaper was designed to follow the profile of this vena contracta, adjusted to give a balance between the dimensions of the device and its effectiveness. The maximum convenient length of wooden panel (1.2m) to construct the flow shaper suggested the total length. The profile was adjusted to keep the lowest point of the new flow shaper at the agreed outlet opening. The last adjustment concerned the part of the shaper inside the tank, simplified as water movement in the tank didn't require a curved profile.

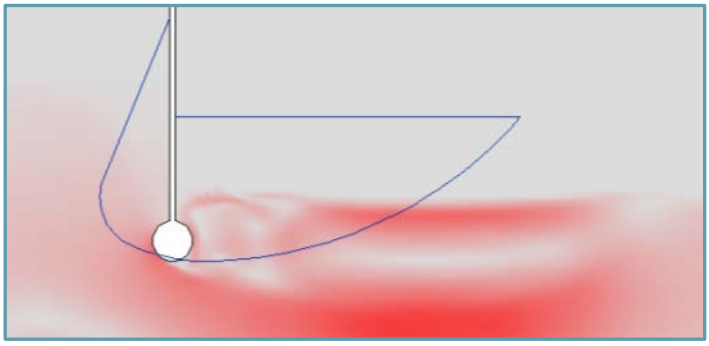

Figure 13: Final design of the new outlet flow shaper, adjusted both in dimensions and position

3.5 Running tsunami traces

The transfer functions studied earlier used super-imposed hyperbolic tangents. Generation of time series from tsunami records came as a second stage. These require time series of surface elevations, but digitised signals were not available for any tsunami. Even for the Mercator signal; it was necessary to scale surface elevations in time from a photograph of the original paper record. For a tsunami to be modelled at 1/50, surface elevations were divided by 50 and time by √50. Pressures were calculated using transfer functions deduced for trough and crest.

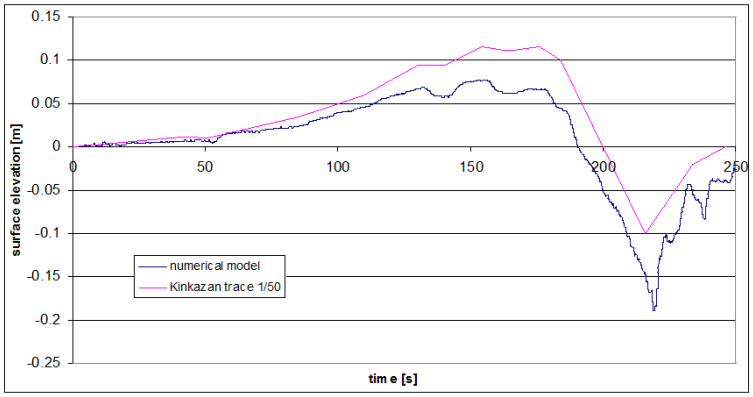

Figure 14a: Kinkazan trace at 1/50, using simplified time series (simulation G6.M1.W3.il_3)

Initial tests to model the trace for Kinkazan (Figure 14a) confirmed the need for improved transfer functions as the scaled crest of the real Kinkazan tsunami was 0.116m high, 50% more than the one numerically reproduced (0.077m). The trough was also deeper than it should be, probably because of the smaller crest.

This was followed by re-creating a simplified version of the Tohoku GPS signal (Figure 3b) at 1/50 using updated transfer values. The results are initially encouraging. The height reached for the longer first component matched the requirement. The second stage 'spike' was however delayed, but did exceed the desired height, but this might have been due to the returning reflected wave. Two unexpected peaks were present later in the signal and it is again plausible that these were due to reflections.

3.6 Pressure inputs from physical model

In the last stage of this study, the numerical model was run to assess its ability to replicate measured phenomena. Tank pressure time series recorded during the physical experiments, became inputs to numerical simulations. Results of one of these simulations are illustrated in Figure 14b, compared with surface elevations from the physical flume.

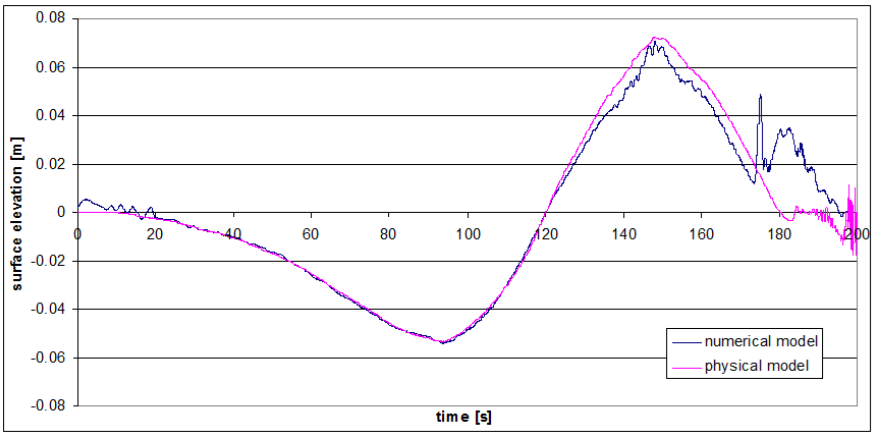

Figure 14b: Mercator trace at 1/50 scale, comparison between physical and numerical model, using measured tank pressures as input for simulation G6.M1.W3.il_7

The agreement of the two curves is excellent in the first half (the trough). There is a slight difference in the crest; the peaks take place at the same time, but the numerical crest is slightly smaller. It was however noted that the approach bathymetry in the physical flume was further from the tank than in the numerical model, and the flat area had been abbreviated in the mesh of the numerical model. The reflected wave therefore happened earlier in the numerical model than in the physical one. So, considering the influence of the different geometries, this comparison was considered satisfactory.

4 Physical modelling

A set of physical tests in 2012 were made opportunistically to explore modifications to the Tsunami Generator and to test the capabilities of the device. Real tsunami traces were then reproduced using information gathered above. In contrast to 2009, the tank was placed in the flume elevated on 0.1m thick concrete blocks, thus raising the roof level to 1.9m, and increasing the available water column to drive the experiments. As before, the Tsunami Generator tank was installed in front of the wave paddle at the end of the flume so the active length of the flume was approximately 40m.

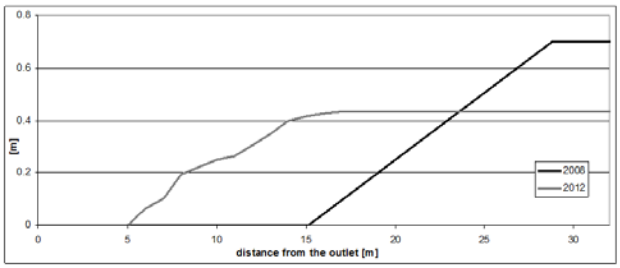

Figure 15: Bathymetries used for physical modelling in 2009 and 2012

The bathymetry of the flume in 2012 was significantly different from that used earlier (Figure 15). Following on from the numerical modelling described above, the outlet was revised. The aperture height was 0.25m, and the lip was reshaped as in Figure 13. The profile was formed by three arcs of 0.15, 0.5 and 1.2m of radius and a straight segment inside the tank to join the curves of the flow shaper to the inner tank panel. A water level gauge inside the tank, recorded information on TWL changes, and another channel recorded the control valve opening. Pressures in the tank were recorded from a transducer mounted in the tank roof.

The experiments used 5 wave gauges, to record flume water levels in different positions. Three of them were placed at 1.2m, 3.3m and 5m from the tank. The others were installed on the slope. Special attention was given to calibrating these gauges because depths on the slope are very shallow, normal calibrations can easily lead to truncation of the peaks.

4.1 General capability testing

In 2009, the study had been focused on generating waves of known profile (sine waves, N-waves and solitary waves). In 2012 more basic capabilities were tested, particularly the limiting capabilities in generating crests and troughs. Later, families of N-waves were generated. Finally real tsunami traces (Tohoku and Mercator) were explored at 1/50 scale.

The first tests were of sudden opening or closure of the air valve to identify the limiting capacity of the device, obtained by operating the control valve at the maximum speed possible. The tank was filled to the top, starting from a half-open control valve position. Then the water was released by opening completely the control valve until the tank reached the lowest TWL practical. In the third phase, the water was lifted again to the upper limit, till the roof, this time starting from the lowest TWL possible. Results are reported for experiments conducted in different positions of the safety valve (both 3º and 0º). For first phase, the starting TWL was about 1.3m. As expected, the highest TWL (about 1.8m) was reached with the safety valve completely shut. These tests with the safety valve in 0º position were repeated (tests O.003.b.1 and O.003.b.2). The excellent agreement of the results (the lines fall completely on top of each other) suggests excellent repeatability of the experiments. The 3° valve experiment illustrates the effect of a partly shut control valve with a slower rise in the tank to a lower final level.

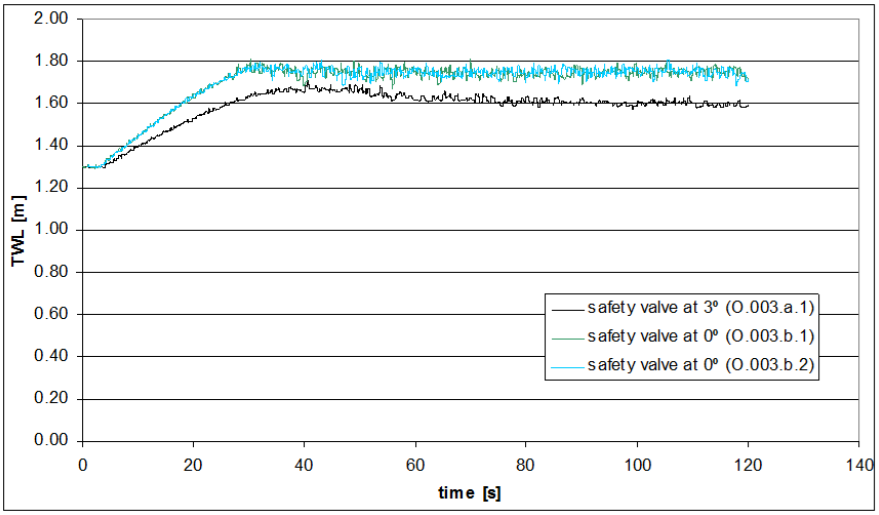

Figure 16: TWL during sudden water suction, starting from partially-open valve

The second phase compared the fall in TWL for a suddenly opened control valve. Here the results overlapped perfectly except for the small difference in starting level for 0° or 3°on the safety valve. After these first few seconds, the curves for TWL show a steady fall to about 0.8m. After this, the curve flattens. It is therefore essential to stay on the first part of this curve when generating a crest. These results support the theory that a higher tank than the current would give better results in crest generation, although it may require a vacuum pump of greater (pressure) capacity. Lastly, the tests shows that the minimum TWL achievable was about 0.6m, about 0.2m above FWL, giving a range of TWL between 0.6m and about 1.8m.

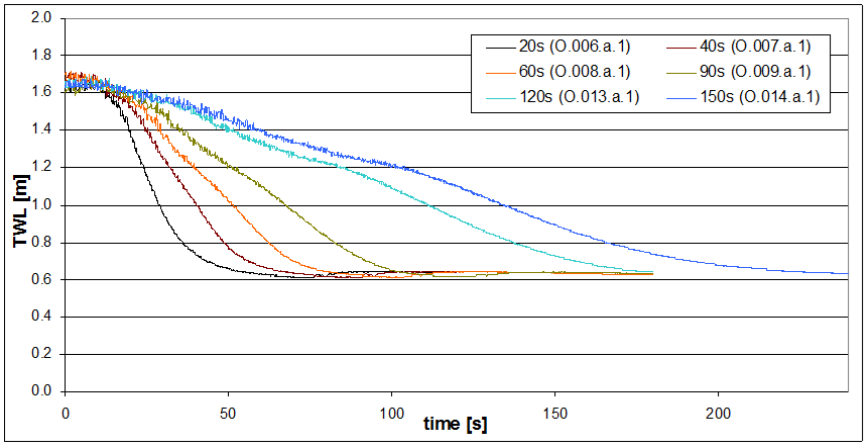

Figure 17: Controlled releases of TWL

Further experiments opened the control valve at different rates, primarily to identify the steepness of the generated crests. The controlled release tests were repeated six times, each with a different duration from 20s to 150s, measuring: valve opening, air pressure, TWL movement and surface elevation in the flume. The process resembles that for sudden release, again with fairly linear fall of the TWL over the central part of the test, Figure 17.

The reverse process was similarly tested with the rate of rise of crests in the flume following mostly linear trends. It had been expected that longer waves would require larger volume to generate the same height. It

was noted that waves generated at different rates reached almost the same height in the flume, especially the shorter ones, with only a little trend that longer waves gave lower peaks.

4.2 Generating N-waves

After testing the limits of the device and its abilities at different generating rates, the research focused on the study of N-waves. The desired N-waves were trough-led with the trough and crest approximately symmetric. From the numerical modelling work on transfer functions, it was expected that a crest would require greater valve movement than the equivalent trough. The starting valve opening was set to 33% open, holding the starting TWL at 1.3m. The first operation of the valve was a slow closure until the "fully shut" condition. The valve was kept in this position for a few seconds to develop the trough in the flume before generating the crest. The release followed, until the "fully opened" condition. The crest required a short period to guarantee a less disturbed peak. The valve eventually returned to 33% to pull water back into the tank, thus generating the tail of the crest. In the first experiment the valve had a closure phase about 45s long followed by an opening phase of about 80s, for a total of 125s. This was then replicated with different durations, stretching or compressing the time series and keeping the same percentages of valve opening. Four experiments fall into this family of "N-waves stretched in time", from 80 to 160 seconds (see Figure 18).

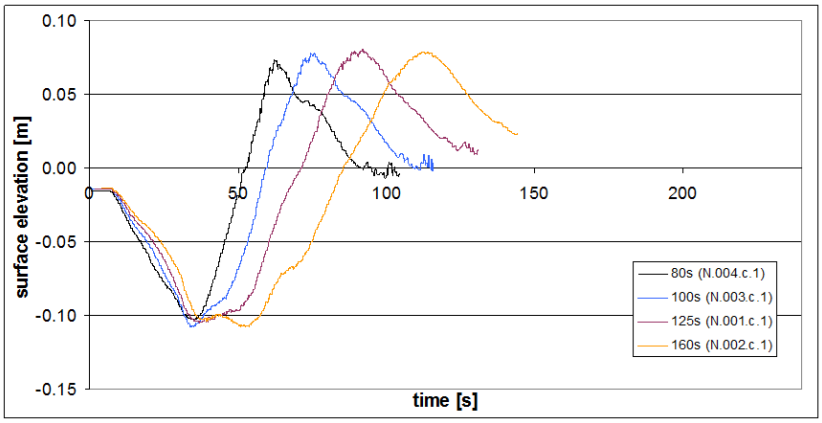

Figure 18: Surface elevations at 1.2m from the tank, depth 0.44m, N-waves of 80-160s T

4.3 Reproduction of tsunami traces

Some of the real tsunami traces available were re-created using the knowledge from the study of general capabilities above. The primary traces were Mercator (Thailand, 2004) and Tohoku (Japan, 2011). The key information observed were steepness and crest / trough amplitudes. Valve opening commands were derived from the nearest test above, for best fits between two tests, modified until the amplitude of the desired wave was reached. Results achieved at the first attempt were usually not far, but a few "trial and error" steps were needed to reach good agreement in height and duration.

Mercator trace is relatively close to one of the N-waves explored above. Knowing amplitudes of trough and crest (-2.8m and 3.7m in prototype) and their steepness, valve opening times were identified from the controlled suction-release experiments. A couple of adjustments were necessary to improve the shape of the trough. The final result was however very satisfying and the agreement with the Mercator digital signal was very good through the trough and almost perfect at the crest.

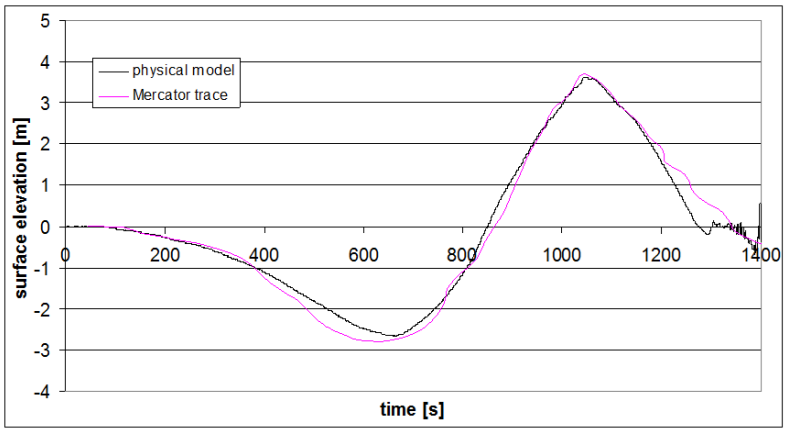

Figure 19: Mercator trace at 1/50 scale (test T.013.a.1)

Re-creation of the Tohoku trace was more challenging. The first wave is long but relatively low, so it was hard to identify the valve time series to generate the correct profile. The second wave, a 3m high peak, takes the generator to the limits of its ability, both on the rise and fall over the upper peak. The valve closure was very fast but the TWL was not able to rise with the desired speed and followed a less steep profile.

Figure 20 shows the values of the surface elevation (scaled to prototype) recorded by the first wave probe, located at 1.2m from tank's frontal panel. Reflection aside, the results are quite satisfying considering that the height of the first wave reaches exactly 2m before the peak and the peak itself is just a bit shorter than the desired 5m. Nevertheless this Tohoku re-creation can be further enhanced, especially in the extent of the high peak. Despite the problem of the descending part of the high peak (insufficient speed in the increase of TWL) it seems that also that part of the wave was quite well reproduced.

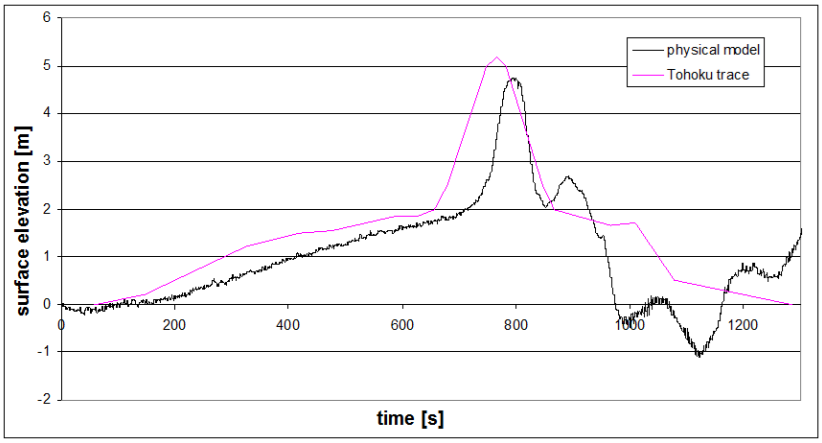

Figure 20: Tohoku trace at 1/50 scale (test T.008.a.1)

Acknowledgements

The work reported here was substantially conducted by Alice Barthel (Visiting Researcher from Ecole Central de Lyon) and Mario Zaccaria (Visiting Researcher from University of Padua), based on advances by David Robinson (2009) and Ingrid Charvet (2011). This paper was (in part) compiled from reports by Barthel and

Zaccaria supported by HYDRALAB IV under HyRes topic 9.1.2. Additional material has been generated under the URBANWAVE ERC project between UCL and HR Wallingford.

References

Allsop W., Robinson D, Charvet I, Rossetto T. & Abernethy R (2008) “A unique tsunami generator for physical modelling of violent flows and their impact”, Proc. 14th World Conference on Earthquake Engineering , October, Beijing.

Barthel, A. (2011). Improving tsunami wave generation, Technical Note No. DDS0336-01 for HYDRALAB HyRes 9.1.2, HR Wallingford.

Charvet I (2011) Experimental modelling of long elevated and depressed waves using a new pneumatic wave generator, PhD thesis, University College London,

Hammack, J. L. (1972), Tsunamis - a model of their generation and propagation, Rep. KH-R-28, W. M. Keck Lab. of Hydraulics and Water Resources, California Inst. of Technol., Pasadena

Madsen, P. A., Fuhrman, D. R. & Schäffer, H. A. (2008). On the solitary wave paradigm for tsunamis. Journal of Geophysical Research, 113.

Penchev, V. (2009). Extreme Solitary waves at restricted water depth. Proc. of Coastlab08 – 2nd Int. Conf. on Application of Physical Modelling to Port and Coastal Protection, pp. 335-340, ISBN: 978-90-78046-07-3, publn. IAHR, Madrid.

Robinson, D. (2009). Development of the HRW Tsunami Generator: Conceptual design and preparatory modelling studies (IT585), HR Wallingford.

Rossetto, T., Allsop, W., Charvet, I. & Robinson, D. (2011). Physical modelling of tsunami using a new pneumatic wave generator. Coastal Engineering, 58(6), pp. 517-527.

Russel, J. S. (1845). Report on Waves. Report of the 14th meeting of the British Association for the Advancement of Science, pp. 311-390.

Schmidt-Koppenhagen, R., Grune, J. & Oumeraci, H. (2006). Tsunami wave decay in near and onshore areas. ICCE, 2, pp. 1664-1676.

Tadepalli, S. & Synolakis, C. E. (1994). The Run-Up of N-Waves on Sloping Beaches. Proceedings of the Royal Society A, 445(1923), 8 April, pp. 99-112.

Thusyanthan, N. I. & Madabhushi, S. P. (2008). Tsunami wave loading on coastal houses: a model approach. Proceedings of the Institution of Civil Engineers. Civil Engineering, 161(2), 1 May, pp. 77-86, ICE, London.

Titov, V. V. & Synolakis, C. E. (1998). Numerical Modeling of Tidal Wave Runup. J. Waterway, Port, Coastal, Ocean Eng., 124(4), pp. 157-171.

Wiegel, R. L. (1955) Laboratory studies of gravity waves generated by the movement of a submerged body. Trans. AGU 36, 759–774.

Yim SC, Cox DT & Park MM (2009) Experimental and Computational activities at the Oregon State University NEES Tsunami research Facility, Science of Tsunami Hazards, 28(1), pp1-14.